



HAL
open science

Full-scale fire test on a high-rise RC wall

Duc Toan Pham, Nicolas Pinoteau, Mingguan Yang, Patrick de Buhan, Pierre Pimienta, Romain Mège

► **To cite this version:**

Duc Toan Pham, Nicolas Pinoteau, Mingguan Yang, Patrick de Buhan, Pierre Pimienta, et al.. Full-scale fire test on a high-rise RC wall. *Engineering Structures*, 2021, 227, pp.111435 -. 10.1016/j.engstruct.2020.111435 . hal-03492682

HAL Id: hal-03492682

<https://hal.science/hal-03492682v1>

Submitted on 10 May 2022

HAL is a multi-disciplinary open access archive for the deposit and dissemination of scientific research documents, whether they are published or not. The documents may come from teaching and research institutions in France or abroad, or from public or private research centers.

L'archive ouverte pluridisciplinaire **HAL**, est destinée au dépôt et à la diffusion de documents scientifiques de niveau recherche, publiés ou non, émanant des établissements d'enseignement et de recherche français ou étrangers, des laboratoires publics ou privés.

Full-scale fire test on a high-rise RC wall

Duc Toan Pham^{1,*}, Nicolas Pinoteau¹, Mingguan Yang^{1,2}, Patrick de Buhan², Pierre Pimienta¹, Romain Mège¹

¹ Université Paris-Est, Centre Scientifique et Technique du Bâtiment (CSTB), 84 avenue Jean Jaurès, Champs-sur-Marne, 77447 Marne-la-Vallée Cedex 2, France

² Université Paris-Est, Laboratoire Navier (Ecole des Ponts ParisTech, IFSTTAR, CNRS UMR 8205), 6-8 avenue Blaise Pascal, Cité Descartes, Champs-sur-Marne, 77455 Marne-la-Vallée Cedex 2, France

* **Corresponding author:** Duc Toan Pham

Email: ductoan.pham@cstb.fr

Tel : +33 1.61.44.81.89

ABSTRACT

This paper describes a *full-scale* test carried out on a high-rise reinforced concrete wall subjected to fire loading conditions in the special Vulcain furnace (very large and modular gas furnace) at CSTB, France. The test sample was designed to represent a slender wall with a very large height/thickness ratio. The experimental results showed a large deflection of the high wall in fire conditions (almost equal to the wall height/24) even for a fire exposure time of 90 min. Such a deflection was significantly higher than the maximum value recommended by design codes (about the wall height/30 for 120 min of fire exposure). Furthermore, other test results (full-field displacements in the 3 directions, residual deformed shape after the heating and cooling phases) may also provide additional useful experimental data for validating available or future models (which are usually based on some specific assumptions). In addition, the measurements of thermal-induced deformed shape of the wall are compared to

those predicted by an analytical solution derived from a simplified one-dimensional (1D) beam model, as well as to those obtained from non-linear finite-element simulations (with 2D plate elements), in order to assess the practical applicability of these simulations. These comparisons show a reasonably good agreement between the experimental results and the predictions of these models, thereby providing a first validation of the latter.

Keywords: full-scale test; fire loading; high-rise wall; large deflection; reinforced concrete.

1. INTRODUCTION

A great amount of tests has been carried out after about a century of investigations on the fire resistance of structures under standard conditions. One may quote, among many others, the experiments performed by Lie and Woollerton [1]; Dotreppe *et al.* [2]; Franssen and Dotreppe [3]; Kodur and Mcgrath [4], who more specifically focused their attention on the fire resistance of reinforced concrete (RC) columns exposed to fire; the fire tests on unbonded and bonded post-tensioned concrete slabs of Bailey and Ellobody [5, 6] or the experimental work of Crozier and Sanjayan [7] on slender RC walls. However, even though results of these standard fire tests provide useful experimental data for validating theoretical and numerical models, they are still limited to the situations where the dimensions of the tested structural components should remain compatible with those of conventional furnaces (furnace height is about 3 m, while furnace width may reach 4 m). In this context, any attempt to perform a full-scale test on a high-rise structural element requires the use of a higher (and wider) furnace such as the test of Lahouar *et al.* [8]. On the other hand, the large-scale non-standard structural fire testing (see for example Troxell [9], Rubert and Schaumann [10]; British Steel [11], Bailey and Lennon [12], or quite recently Santiago *et al.* [13]) may present an interesting alternative (Bisby *et al.* [14]), but its reproducibility remains questionable.

With an increasing use in industrial buildings, the evaluation of fire behaviour of high-rise RC walls which are larger than the dimensions of conventional experimental test furnaces, requires a more sophisticated approach than for conventional, *i.e.* smaller size structures. Indeed, important out-of-plane (horizontal) displacements due to thermal-induced deformations induce an eccentricity of the vertical load (self-weight) with respect to the initial vertical plane of such the slender wall. Therefore, bending moments are generated in the wall in addition to the pre-existing compressive axial force distribution due to the wall self-weight,

which is usually known as a second order (or *P-delta*) effect (Bazant and Cedolin [15]). Moreover, it is well known that elevated temperatures lead to local degradation of the stiffness and strength properties of both concrete and steel materials, which may accentuate the wall deformations still further.

Based on a simplified one-dimensional (1D) modelling of the problem, a yield design-based approach (Salençon [16]) has been developed for evaluating the potential failure of high-rise RC walls exposed to fire (see Pham [17] or Pham *et al.* [18, 19] for more details). These studies have shown that the equilibrium deformed shape of the wall and the corresponding out-of-plane displacements due to thermal loading, may strongly increase with an even relatively slight increase of its height. On the other hand, the maximum value of $1/30^{\text{th}}$ for the deflection to height ratio (corresponding to a fire exposure of 120 min) recommended in design codes seems to be too conservative for high-rise RC walls. To provide a validation of the previously mentioned theoretical work, a full-scale fire test has therefore been carried out on an 8.4m-high RC wall in the very large and modular furnace Vulcain at CSTB, France.

In the present experimental study, the chosen configuration is the following. The wall is hinged at both ends and the top support can move vertically. This corresponds to a real technological system developed for constructing industrial buildings (see for example CIMbéton [22]). It is obvious that the results obtained in such a configuration, are on the safe side when compared to other configurations, where for instance the bottom of the panel would be clamped instead of simply supported.

According to the tabulated data of EN 1992-1-2 [20] for non-load-bearing partition walls, the ratio of height of wall to wall thickness should be lower than 40 in order to avoid

excessive thermal deformation and subsequent failure of integrity between wall and slab. In the context that such a proposed value was typically based on conventional fire tests (carried out on common structural elements), and in order to extend the specified limits of validity of such design aids for further high-rise walls, the test has been carried out on a slender wall with a very large height/thickness ratio (40% higher than the maximum value recommended in EN 1992-1-2 [20]). Such a heavy and sophisticated fire test may help to reproduce the large deflection and the desired (*P-delta*) effect associated with the large vertical size of the structure, providing thus useful experimental data for validating available or future predictive models (which are usually based on some specific assumptions).

In this paper, the characteristics of the RC wall specimen, the test setup related to its thermal loading and the instrumentation are first described. It would be interesting to note that, in order to gather full-field displacements (in the 3 directions) of the wall during the fire test, a Stereo Digital Image Correlation technique (DIC) was used in addition to classical linear variable differential transformer sensors (LVDTs). The experimental results are then reported and discussed with reference to the equilibrium deformed configuration of the high wall in relation with thermal loading. Finally, the measurements of the thermal-induced deformed shape of the wall are compared to those predicted by an analytical solution derived from a simplified 1D beam model previously mentioned (Pham [17] or Pham *et al.* [18, 19]) as well as to those obtained with non-linear finite-element simulations (with 2D plate elements), in order to assess the validity of these models.

2. TEST PROCEDURE

2.1. Characteristics of the test wall

The RC wall was 2.6m-wide, 8.4m-high and 0.15m-thick, the height being equal to three times the width and the height/thickness ratio being equal to 56. Table 1 presents the concrete formulation which was used. In order to prevent spalling of concrete due to fire, polypropylene fibers were included in the concrete. After 90 days of curing in ambient laboratory conditions, the concrete presented a compressive strength of $f_c = 36.1$ MPa (determined from compressive tests performed on $150 \times 150 \times 150$ mm³ cubes) and a tensile strength of $f_t = 2.75$ MPa (determined from splitting tests on 160×320 mm² cylinders).

Tab. 1. Concrete mix design

Components	Quantity (kg/m ³)
Cement CEM III/A 42.5 N CE CP1 NF	300
Sand silico-calcareous 0/4	802
Aggregates calcareous 4/20	936
Water	170
Superplastizer	1.5
Air entrainer	0.12
Polypropylene fibers (12 mm)	2.82

The wall was reinforced by two symmetrical layers of 9 mm diameter hot rolled steel reinforcing bars of yield stress $f_y = 480$ MPa, ultimate strength $f_r = 533$ MPa and Young modulus's $E_s = 210$ GPa, with a spacing of 100 mm (Fig. 1). The steel bars were arranged in two orthogonal arrays and placed with 25 mm of concrete cover at both the top and the bottom parts of the wall thickness.



Fig. 1. Sample formwork and reinforcement layout of the test wall

2.2. Test setup

The boundary conditions were such that both ends of the wall were articulated (no deflection but free rotation) as shown in Fig. 2. The bottom end of the wall was kept fixed in vertical and transversal translations, while its top end was free to translate vertically. The lateral sides of the wall were stress free. To ensure such boundary conditions, the main part of the wall (8m-high) was connected at the top and the bottom to two concrete blocks of $0.3 \times 0.3 \times 2.6 \text{ m}^3$ which were reinforced in order to resist to concentrated local stresses and connected to the main wall by reinforcing bars. These reinforcing bars were welded to the steel frames (diameter 9 mm) inside the wall. These two concrete blocks were casted before the main wall. A rough surface on the concrete was realized at the interface between the main wall and the concrete blocks (Fig. 3).

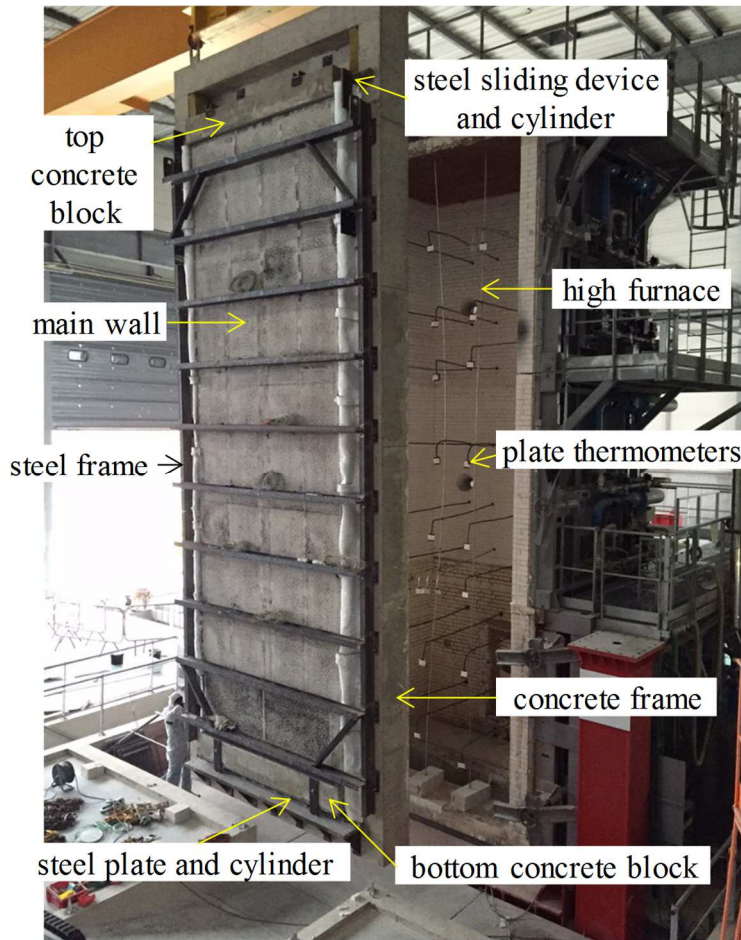
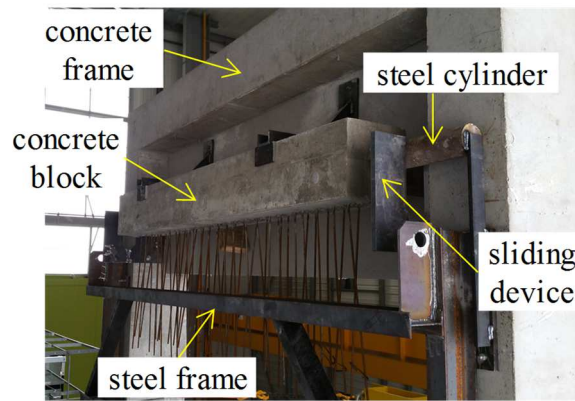


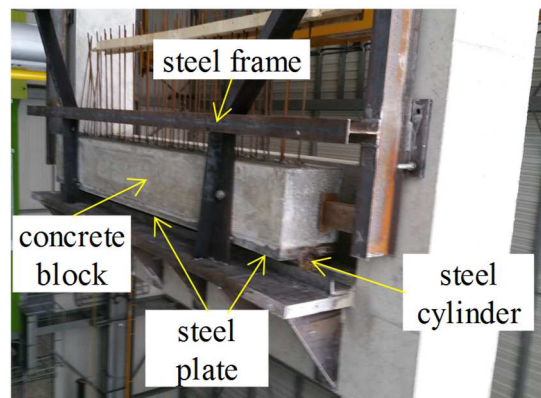
Fig. 2. Positioning of the test sample in front of the furnace

The concrete block at the top (Fig. 3(a)) included a steel cylinder of diameter 100 mm, positioned at mid-width and extended outside the concrete on both lateral sides. The outer parts of this cylinder were used to ensure the boundary condition at the top of the wall (free rotation and vertical translation).

The concrete block at the bottom (Fig. 3(b)) was equipped with a steel plate (20 mm-thick) that was connected to the concrete during casting with steel bars. At mid-width, this plate was equipped with a welded steel cylinder to ensure the boundary condition at the bottom of the wall (free rotation).



(a)



(b)

Fig. 3. (a) Top and (b) bottom concrete blocks before casting of the main wall

The total mass of the sample (main wall and 2 concrete blocks) was around 8 tons. The whole wall was positioned inside a concrete frame for transportation (including retrieving the sample after the test) to place the sample in front of the furnace. This concrete frame (with the sample inside) was used to close the furnace while exposing the sample on one side. Between the sample and the frame, insulating material was positioned to prevent any thermal action on the lateral sides of the wall. This isolation was placed with a fold so as to allow large deflections of the wall without ripping the insulation.

The concrete frame was also used to position the outer mechanical systems ensuring the boundary conditions. At the top, two U-shaped steel devices allowed the steel cylinder to slide

vertically (ensuring translation and rotation- Fig. 3(a)). At the bottom, a steel plate notched at mid-width along the entire length allowed the bottom cylinder to be maintained in position (ensuring the rotation - Fig. 3(b)).

In addition, a steel frame was bolted onto the concrete frame. This steel frame (composed of 2 vertical HEA160 and 10 horizontal HEA100) was used for safety purposes in order to maintain the sample in case of collapse. Flexible steel wires were bolted to the wall samples and connected to the steel frame to prevent the wall from falling in case of failure during the test. The wires were left loose enough (600 mm) to avoid disturbing the deflection of the wall during the test. Finally, the steel frame was used to fix the displacement LVDTs, serving as reference for all the displacements that were measured.

During the fire test, the inner inside surface of the wall was exposed to ISO 834-1 fire (EN 1991-1-2 [21]) for 90 min. The special 9m-high furnace presented a maximal power around 12 MW. The ISO 834-1 curve was conventionally controlled by using 24 plate thermometers positioned at 100 mm from the exposed surface of the test sample. Furnace temperatures were recorded during the test.

2.3. Instrumentation and measurements

The temperatures (across the wall thickness - Fig. 4) of concrete material were measured with thermocouples positioned at different locations (T1 to T8 : Fig. 5). These thermocouples were placed in the central area of the wall as well as in the areas near the lateral sides, as shown in Fig. 5.

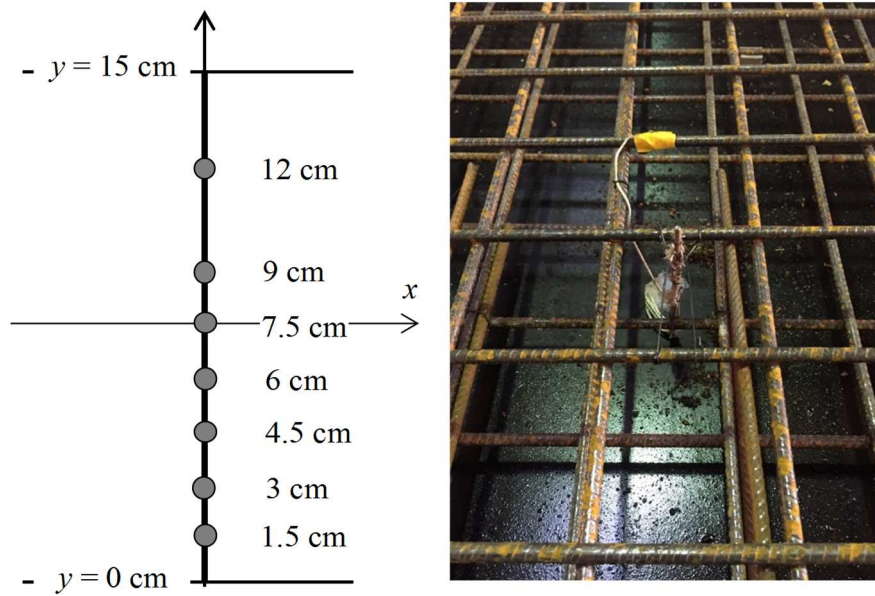


Fig. 4. Thermocouples positioned at different depths across the wall thickness

During the fire test, the resulting displacement evolution was continuously recorded by a data acquisition system. The measurement of the displacement was performed by means of 10 LVDTs along the length of the wall: LVDTs D1 to D9 for horizontal displacements and LVDTs V for vertical displacement of the top of the wall. These LVDTs were fixed on the rigid frame and connected with the non-exposed side of the wall.

In order to avoid edge effects, thermocouples and LVDTs were all placed with a minimum distance of 500 mm from the vertical sides of the wall (see Fig. 5). In addition, the displacement fields in the 3 directions of the wall during the fire test were recorded with a Stereo Digital Image Correlation technique (DIC). The image correlation was carried out using 2 cameras with a resolution of 2.3 MPixels and positioned 7.5 m away from the wall. These two cameras were calibrated to recognize spatial positions by triangulation. To identify displacements, a speckle (composed of black dots presenting a non-uniform distribution and a given diameter) was painted on the non-exposed side of the wall sample.

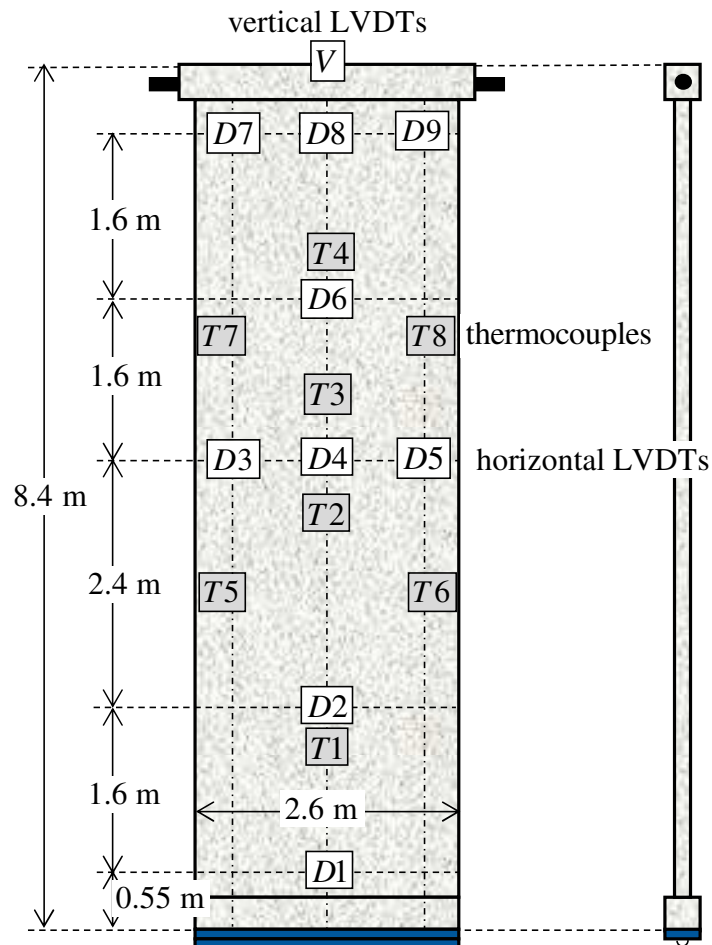


Fig. 5. Positions of thermocouples and LVDTs

3. TEST RESULTS AND DISCUSSIONS

3.1. Thermal loading

The ambient temperature at the beginning of the fire test was recorded with the average values around 13°C. The evolution of the average furnace temperatures in comparison with the ISO 834-1 temperature-vs-time curve (EN 1991-1-2 [21]) is presented in Fig. 6, showing that the applied temperature on the interior surface of the wall closely followed the target ISO 834-1 curve, except for an overshoot in the early stages of the test.

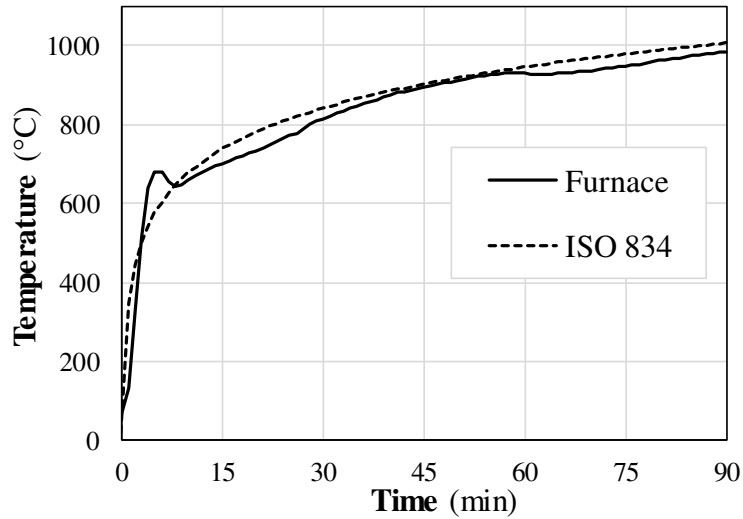


Fig. 6. Average furnace temperatures and ISO 834-1 temperature curve

Figure 7 shows the average temperature profiles across the thickness of the wall, corresponding to 30, 60 and 90 min fire durations. Slightly higher temperatures can be observed in the central zone (thermocouples from T1 to T4) with respect to those in the lateral zone (thermocouples from T5 to T8). For the steel reinforcing bars, since their diameter was small, their temperature could be considered as corresponding to that of the concrete located at the same position (EN 1992-1-2 [21]).

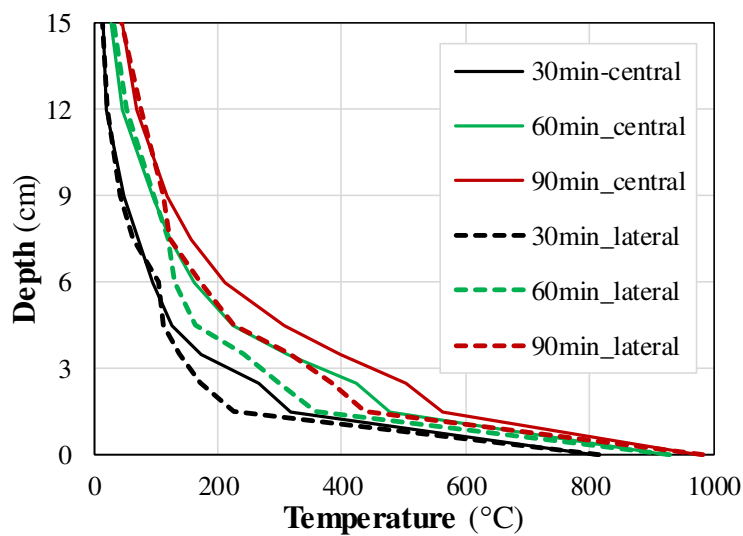


Fig. 7. Average temperature distributions across the wall thickness for different fire exposures

3.2. Live viewing of the wall deflected configuration

During heating, the deformation of the high wall under the combined action of thermal loading (thermal curvature and thermal expansion) and the wall self-weight was clearly visible. Figure 8 displays the out-of-plane deflected shape of the wall after 90 min of fire exposure time. Large displacements were observed, with the maximum value up to 350 mm in the middle-height of the wall. This leads to a deflection/height ratio equal to $1.25/30$ which is 25% higher than the value quoted in design codes, even for a fire exposure time of only 90 min (value of deflection/height around $1/30$ for a fire exposure time of 120 min). However, despite such relatively large deflections, no lateral instability or damage of the structure has been observed.



Fig. 8. Deformed shape of the wall after 90 min of fire exposure time

3.3. Recorded displacements by LVDTs

The displacement vs. time curves are now plotted to investigate the thermo-mechanical behaviour of the whole structure. The corresponding horizontal displacement evolutions recorded by the LVDTs D1 to D9 placed at different locations over the wall height (see Fig. 5) are reported in Fig. 9, positive values corresponding to a movement toward the furnace. The results showed that the measured horizontal displacements as function of fire exposure time was almost linear from the beginning of fire to 10 min and from 10 min to 90 min.

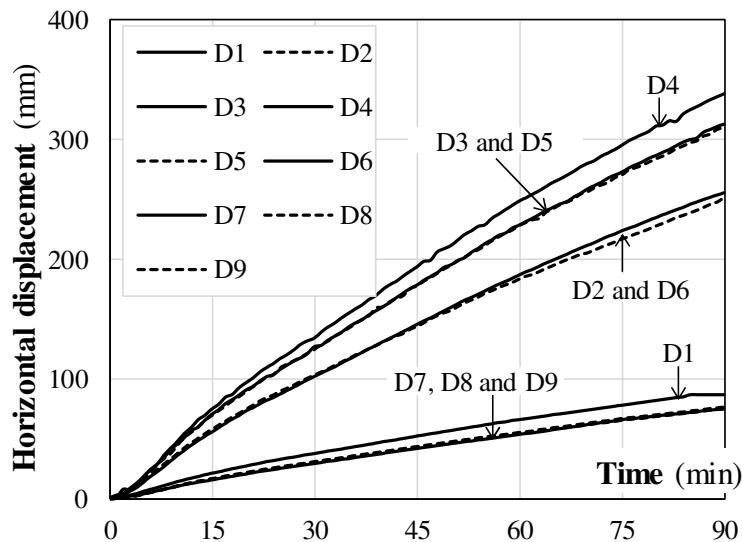


Fig. 9. Evolution of horizontal displacements measured by LVDTs

Focusing more specifically on the three LVDTs D3, D4 and D5 which were in the central area and at the same height of the wall, the maximal displacement was recorded by the centrally located LVDTs D4. The measurements recorded by the two LVDTs D3 and D5 are very close, due to the symmetry of their positions with respect to the vertical central axis of the wall. As described in more details in the following section, this indicates that the thermal gradient over the wall thickness induces horizontal as well as vertical thermal curvatures.

Values recorded by the three LVDTs D7 to D9 were lower and very close since they are placed near the top edge of the wall. Moreover, the edge was connected to the concrete block (Fig. 3(a)) and simply supported, thus preventing out-of-plane displacement at the top edge.

Figure 10 shows the evolution of the vertical displacement measured by LVDTs V (placed at the top of the test wall - Fig. 5) as a function of the fire exposure time, positive displacements corresponding to a downwards movement. As can be seen from this figure, the top of the wall is first moving upwards due to thermal expansion, then after 15 min moves in the opposite direction (*i.e.* downwards) as the thermal curvature and related out-of-plane displacements increase.

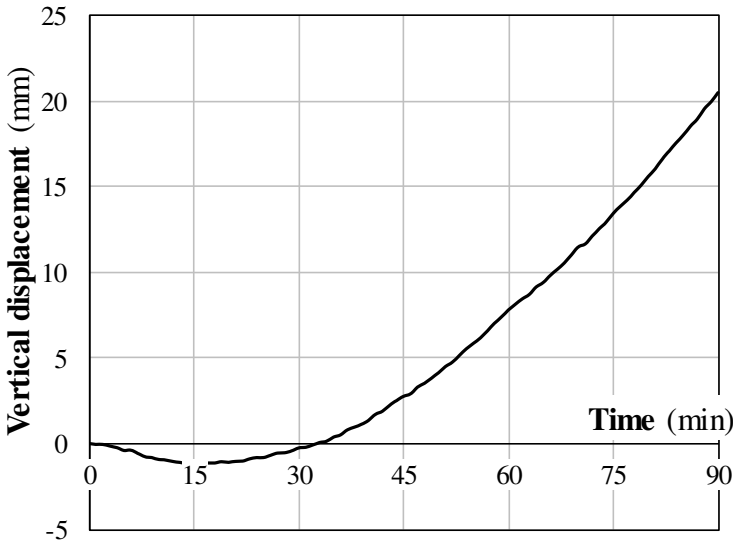


Fig. 10. Evolution of vertical displacements (counted positive downwards) measured by LVDTs at the top of the wall

3.4. 3D deformed shape obtained by image correlation technique

Figure 11(a) shows the contours of the out-of-plane (horizontal) displacements of the wall obtained by Digital Image Correlation technique after 90 min of fire exposure, while figure 11(b) presents the associated 3D deformed shape (the negative displacements are

oriented towards the fire). It must be emphasized that the measurement by Digital Image Correlation technique was very close to the values obtained by LVDTs. The horizontal strips without values are due to the presence of the horizontal steel beams placed in front of the wall (Fig. 8).

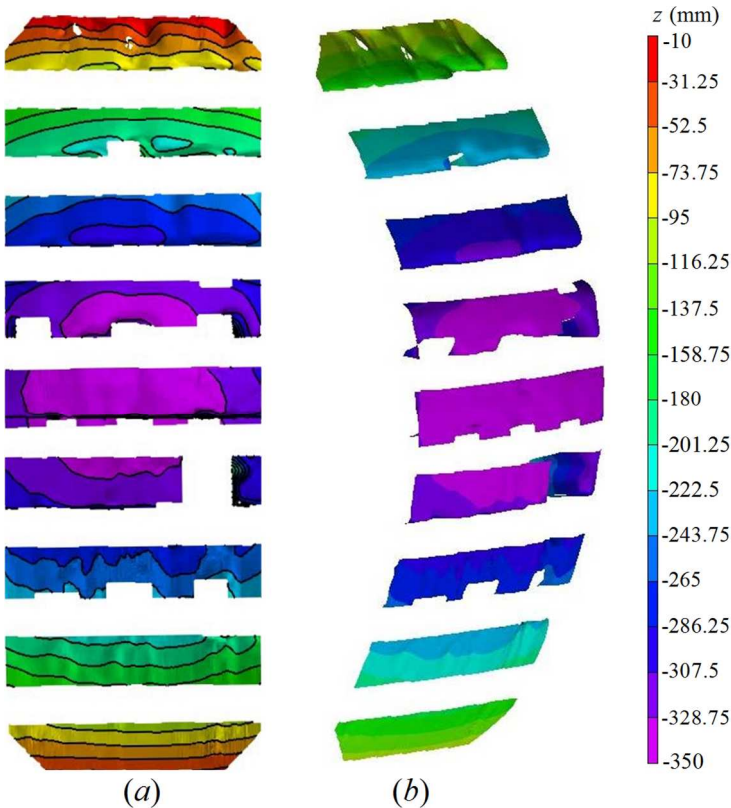


Fig. 11. Contours of the wall horizontal displacements (in mm): (a) front view and (b) 3D deflected configuration of the wall

From Fig. 11, it can be immediately seen that distribution of displacements is almost symmetrical with respect to the mid-height as well as to the mid-width of the wall, with the maximum values appearing in the central zone. The curvatures seem to be slightly decreasing from the central area of the wall to its top and bottom horizontal edges. Moreover, an estimated one third of the wall surface does not seem significantly affected by the conditions on these horizontal end supports (where the out-of-plane displacements were kept equal to

zero during the test). This may be due to the fact that, the width of the wall (2.6 m) is equal to one-third of its height (8.4 m) that is enough to neglect the influence of the two top and bottom edges, while the lateral sides of the wall are stress free.

Figure 12 presents the horizontal displacement profiles along the height near the mid-width of the wall, while figure 13 shows the horizontal displacement profiles along the width at mid-height of the wall, as functions of fire exposure time. Values recorded about 24 h after the end of the thermal loading are also given in these two figures (blue lines). During this cooling phase, the horizontal displacement was reduced to about one-third of the maximum recorded value (110 mm) and did not return to zero (initial vertical plane). This implies that non negligible irreversible plastic deformations have been generated during the fire test. This residual deformed configuration of the wall thus provides additional information on the final equilibrium of the structure after the entire heating and cooling cycle.

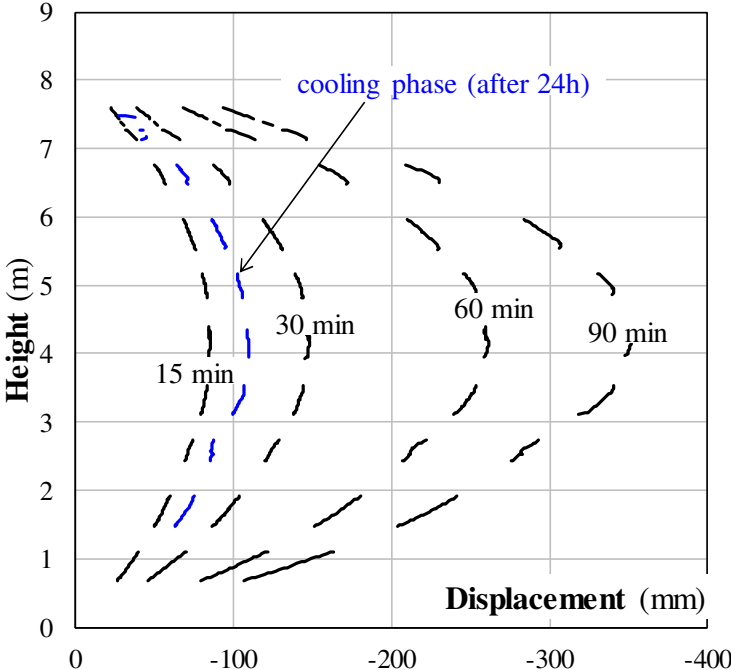


Fig. 12. Horizontal displacement profiles along the height near the mid-width of the wall as function of fire exposure time (note that the horizontal scale is strongly dilated)

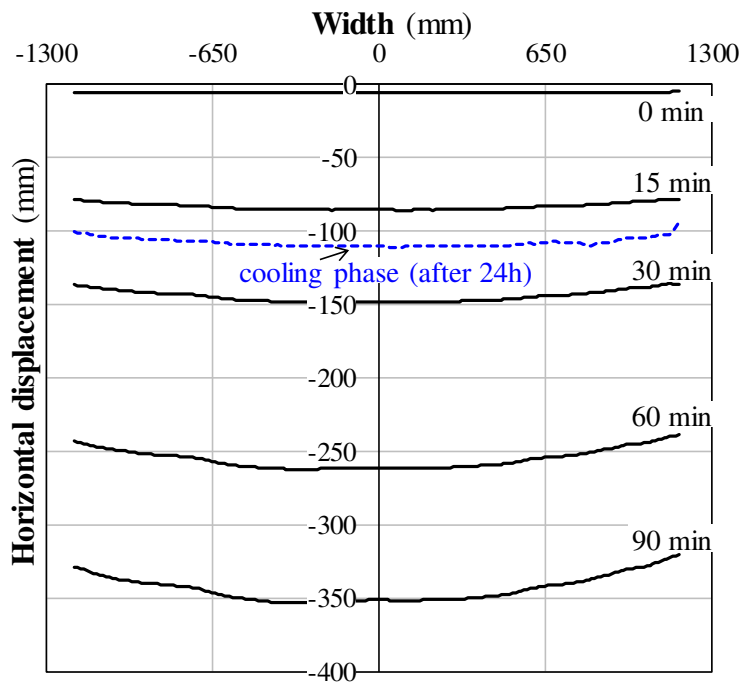


Fig. 13. Horizontal displacement profiles along the width at mid-height of the wall as function of fire exposure time (note that the vertical scale is strongly dilated)

4. COMPARISON WITH AN ANALYTICAL SOLUTION DERIVED FROM A SIMPLIFIED ONE-DIMENSIONAL (1D) BEAM MODEL

In this section, experimental results are compared to those obtained from a simplified one-dimensional (1D) beam model of the high-rise wall, represented as an initially straight vertical beam of height H and thickness h , articulated at both ends as shown in Fig. 14.

A fully detailed description of the theoretical model, with the associated assumptions and the proposed iterative calculation procedure may be found in Pham [17] or Pham *et al.* [18, 19]. The geometric configuration of the high-rise wall is determined from a thermo-elastic iterative calculation accounting for geometrically non-linear second order effects. This calculation is carried out until convergence of the sequence of computed transversal displacements is observed.

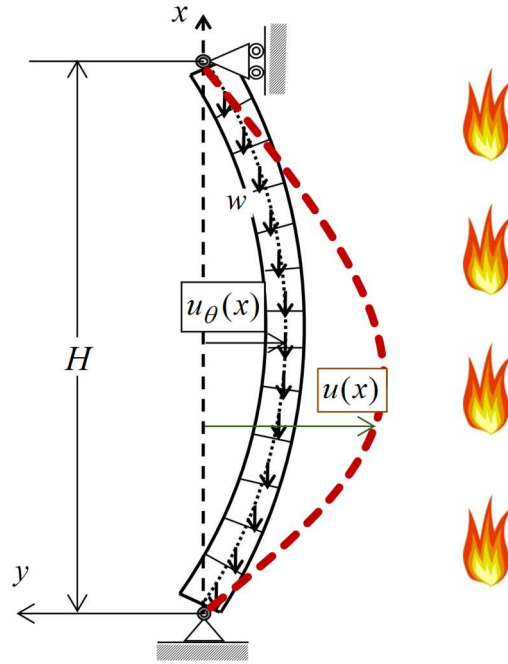


Fig. 14. Schematic diagram of thermal and equilibrium deformed shapes of the wall under fire loading
(Pham [17] or Pham *et al.* [18, 19])

As it has been shown in Pham [19], such an iterative procedure, which could appear time consuming, remains however quite simple since the deformed shapes corresponding to the second and the third iterations are almost coincident with the converged solution. By carrying out 2 iterations of the iterative procedure proposed in these studies, the following closed-form expression of the solution of the final equilibrium deformed configuration of the wall, characterized by the out-of-plane displacement u at any point x , may be obtained:

$$u(x) = \frac{1}{120960} \frac{1}{(EI)_\theta^2} \chi_\theta w^2 f(x) \quad (1)$$

where

$$f(x) = x(H-x)(30x^6 - 162x^5H + 300x^4H^2 - 120x^3H^3 - 239H^4x^2 + 153H^5x + 153H^6) \quad (2)$$

is a polynomial function of degree 8, w denotes the constant linear density of the wall self-weight while χ_θ and $(EI)_\theta$ are the constant curvature of the wall and the wall section flexural stiffness under pure bending, respectively. These quantities may be easily calculated for any prescribed thermal gradient across the wall thickness (see Pham [17] or Pham *et al.* [18, 19] for more details).

For numerical applications of the proposed model, the thermal gradients across the wall thickness were introduced by the use of the temperatures in the central zone provided in Fig. 7. Since the temperature dependencies of the thermal-mechanical properties of concrete as well as steel materials were not directly measured in this work, material properties were considered to be temperature dependent according to Eurocode 2-Part 1-2 (EN1992-1-2 [20]). Besides, in order to include the majority of encountered normal strength concretes and limit the effects of some uncertainties concerning the material properties due to lack of extra characterization tests, material properties of concrete with both siliceous and calcareous aggregates are used for comparison. As a direct result, performing calculation with siliceous aggregates concrete is on the safe side, thus providing an upper bound estimate of the out-of-plane displacement. On the other hand, calculations with calcareous aggregates concrete lead to lower bound estimates.

The results of both experiments and theoretical predictions are illustrated in Fig. 15, showing a rather good agreement between them. As expected, the experimental measurements are located between two corresponding theoretical predictions (lower and upperbounds). This comparison represents a first preliminary validation of the simplified 1D beam model and the associated closed-form expression of the equilibrium deformed configuration, even in the absence of extra characterization tests of material properties of concrete as functions of temperature increase. Besides, the deflection values predicted with siliceous aggregates

concrete are higher than those resulting from the use of calcareous aggregates concrete (the relative difference between the maximum deflections is about 20%). This suggests that the results of the theoretical model are quite sensitive to the variation of the thermal expansion with temperature, $\varepsilon_c(\theta)$, as well as to the coefficient $k_c(\theta)$ quantifying the decrease of stiffness and strength properties of the concrete material as a function of temperature increase (see Pham [17] and Pham *et al.* [19] for more details).

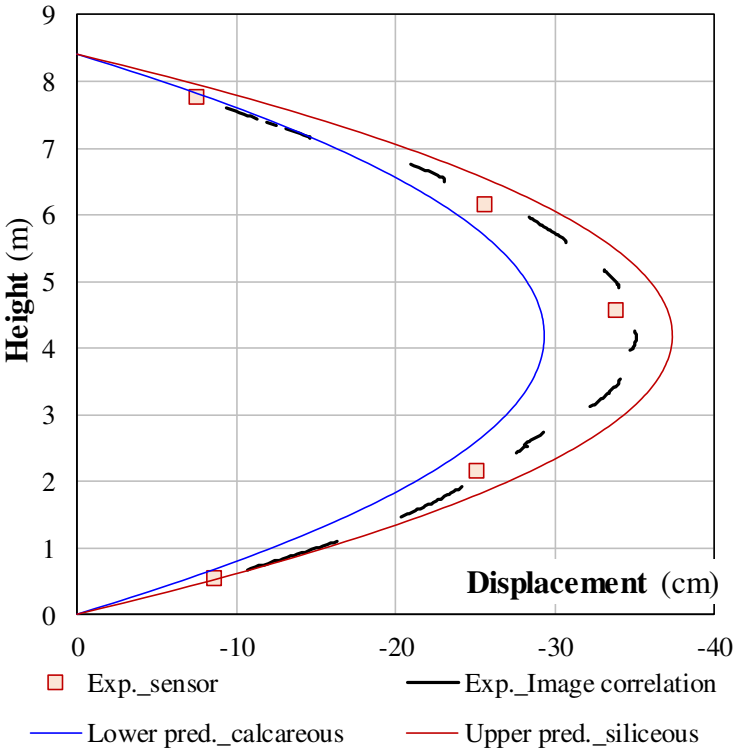


Fig. 15. Comparison of experimental results with theoretical predictions (note that the abscissa scale is strongly dilated)

5. COMPARISON WITH THE RESULTS OF NUMERICAL SIMULATIONS WITH 2D PLATE ELEMENTS

The main limitation of the simplified 1D beam model presented above lies in the fact that the horizontal curvature as well as the vertical displacement of the wall top edge could not be

directly evaluated. Indeed, the wall was hinged along the bottom edge, but it was not hinged along the top edge. In fact, two U-shaped steel devices allowed the outer parts of the steel cylinder of the concrete block at the top of the wall to slide vertically (in order to ensure the free rotation and vertical translation - see Fig. 3(a) for more details). Moreover, the thickness of the two concrete blocks which was twice the thickness of the main wall, may have some influence on the final out-of-plane displacements field. For these reasons, two numerical simulations using a dedicated finite element software (Marc finite-element code - MSC Software Corporation [23]) of the same problem have been performed. These simulations differed from each other by the top and bottom end conditions as summarized in Tab. 2.

Tab. 2. Difference between two numerical simulations (with 2D plate elements)

	Simulation 1	Simulation 2
Boundary conditions at the bottom edge	Hinged	Hinged
Boundary conditions at the top edge	Hinged	Simply supported on 2 points
Concrete blocks at the bottom and top edges	Not simulated	Simulated

The numerical calculation is performed in the context of a thermo-elastic behaviour (see Pham [17] for a detailed description of the specific features of the simulation). For illustrative purpose, the results of the non-linear finite-element simulation for the first wall (wall 1 - without concrete blocks and hinged along two top and bottom edges) are presented in Fig. 16, in the form of the contours of the out-of-plane as well as vertical displacements experienced by the wall for 90 min of fire exposure (values in meters). As expected, the displacements distribution is symmetrical with respect to both the mid-height and the mid-width of the wall, with the maximum value in the central part of the wall.

The corresponding maximum out-of-plane deflections and vertical displacement of the top wall of the simplified 1D and 2D plate models are reported in Tab. 3. It confirms that the influence of both the concrete blocks and the 2 points support on the final maximum out-of-plane displacement is negligible. Besides, the results of the simplified 1D model seems to be on the safe side and accurate enough for a preliminary engineering design of this kind of structure.

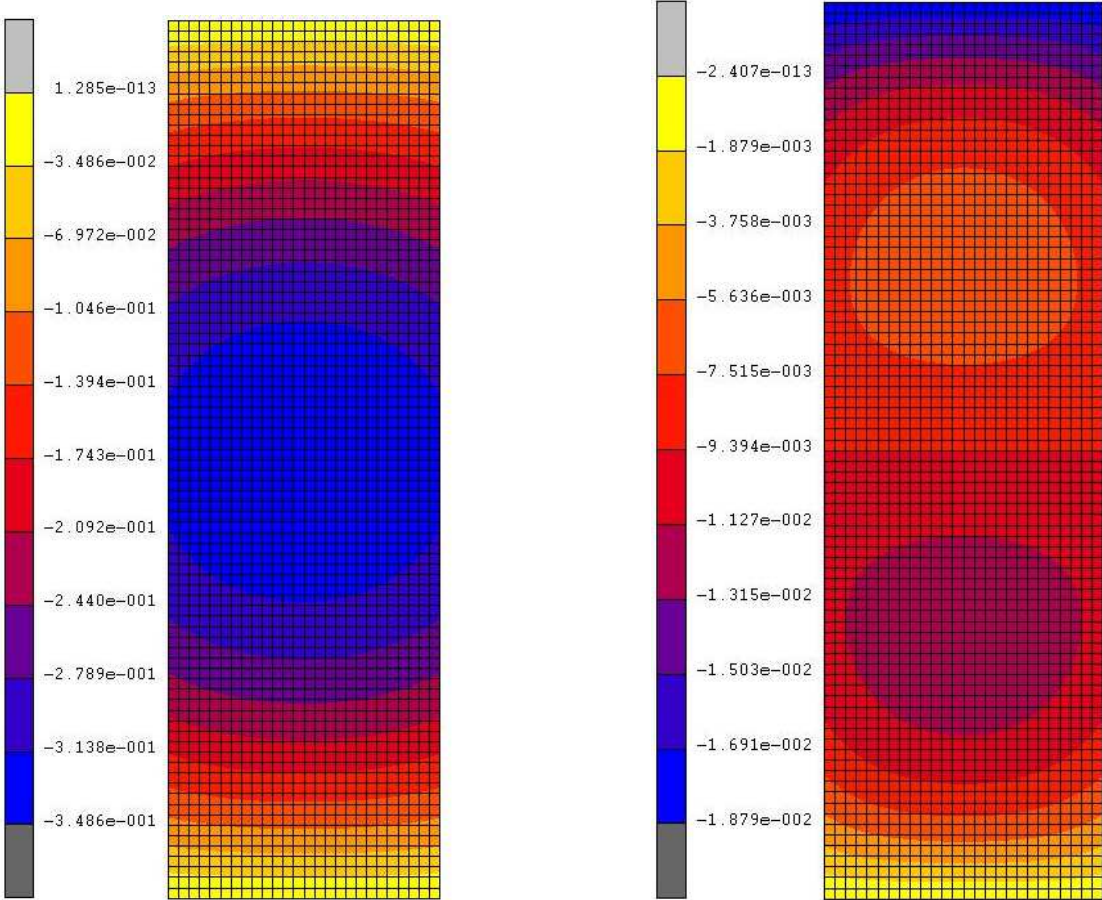


Fig. 16. Face views of contours of the wall out-of-plane (left) and vertical displacements (in meters) (right)

Table 3. Comparison between maximum displacements obtained by the simplify 1D beam model and the 2D plate models

	Vertical displacement of the wall top edge (cm)	Maximal out-of-plane displacements (cm)
1D beam model	Not directly obtained	37.4
2D plate model (without concrete blocks at the bottom and top edges and hinged along the top edge)	1.9	34.9
2D plate model (with concrete blocks and simply supported on 2 points)	2.1	35.4

6. CONCLUSIONS

The purpose of this experimental study was to investigate the influence of temperature increase on the thermal-induced change of geometry of a high-rise reinforced concrete (RC) wall. The full-scale fire resistance test has been successfully carried out on an 8.4m-high wall. The experimental results have shown some specific features of such a full-scale fire test which might affect current design practices as follows:

- The maximum value of 40 relating to the height to thickness ratio of the wall indicated in the design codes (EN 1992-1-2 [20]) seems to be too much restrictive as regards the application of these codes to very slender walls. This is probably due to the fact that the additional horizontal displacement due to further elastic bending associated to the self-weight eccentricity, remains negligible in the case of walls of normal heights. When the ratio of height of wall to wall thickness is higher than 40, geometrically non-linear second order effects should be taken into account.
- The evolution of the deflection of the high wall as a function of the fire exposure time appears to be almost linear. This deflection could reach a much higher value than that

indicated by design codes for walls of normal heights (experimental value around wall height/24 even for a fire exposure time of 90 min compared to a value of wall height/30 for a fire exposure time of 120 min). As a consequence, such a value should be revised for the case of high-rise walls.

- Contrary to walls of normal heights, the top of the high-rise wall is not always moving upwards due to the axial thermal expansion of the concrete material. The wall top edge appeared to be moving downwards as soon as the deflection exceeded a specific value (of the order of the wall thickness (after about 35 min) in the present test). This was due to the fact that the effect of transversal displacement (which is directly linked to the thermal curvature) became more important than that of in-plane displacement (vertical displacement) which was related to the axial thermal expansion.
- At the end of the total heating-cooling cycle, the wall did not return to its initial vertical configuration, which is probably due to irreversible plastic deformations induced by the fire test. Even for only 90 min of fire exposure, the residual out-of-plane deflection may remain important (two thirds of the wall thickness in the present test).

In addition, comparisons have also been made on the deformed shape predicted by a simplified 1D beam model, in which particular importance was attributed to the degradation of material properties under fire-induced thermal loading, as well as by a non-linear finite-element simulation (with 2D plate elements) of the same problem, in order to assess their practical validity. Such comparisons show a reasonably good agreement between experimental and theoretical/numerical predictions, thereby validating the theoretical and numerical models. It confirms that the simplified 1D model provides results on the safe side and accurate enough for a preliminary engineering design of this kind of structure. For the

more realistic 2D plate models, displacement distributions may not be significantly affected by the boundary conditions prescribed along the top and bottom edges (with or without concrete blocks, hinged along the top edge or simply supported on 2 points) if the wall is high enough (the wall height should be three times higher than the width). On the other hand, the results of this unprecedented test may provide useful experimental data for validating available or future models based on some specific assumptions.

ACKNOWLEDGMENT

Authors wish to thank all members of experimental team of the Mechanical and Fire Resistance division at CSTB: Philippe Rivillon, Romuald Avenel, Stéphane Charuel, Jean-Francois Moller, for their help to make the test successful.

REFERENCES

- [1] Lie TT and Woollerton JL. Fire Resistance of Reinforced Concrete Columns: Test Results. IR 569, IRC, National Research Council of Canada, Ottawa, Canada; 1988, 302 pp.
- [2] Dotreppe JC, Franssen JM, Bruls A, Baus R, Vandeveld P, Minne R, van Nieuwenburg D, Lambotte H. Experimental research on the determination of the main parameters affecting the behaviour of reinforced concrete columns under fire conditions. Magazine of Concrete Research 1997;49(179):117-27.
- [3] Franssen JM and Dotreppe JC. Fire tests and calculation methods for circular concrete columns. Fire Technology 2003;39(1):89-97.
- [4] Kodur V and McGrath R. Fire endurance of high strength concrete columns. Fire Technology 2003;39(1):73-87.
- [5] Bailey CG and Ellobody E. Fire tests on unbonded post-tensioned one-way concrete slabs. Magazine of Concrete Research 2009;61(1):67-76.
- [6] Bailey CG and Ellobody E. Fire tests on bonded post-tensioned concrete slabs. Engineering Structures 2009;31(3):686-96.
- [7] Crozier A and Sanjayan JG. Tests of load-bearing slender reinforced concrete walls in fire. ACI Structural Journal 2000;97:243-51.
- [8] Lahouar MA, Pinoteau N, Caron JF, Foret G, Rivillon P. Fire design of post-installed bonded rebars: Full-scale validation test on a $2.94 \times 2 \times 0.15 \text{ m}^3$ concrete slab subjected to ISO 834-1 fire. Engineering Structures 2018;174:81-94.

- [9] Troxell GE. Fire resistance of a prestressed concrete floor panel. *Journal of the American Concrete Institute* 1959;56(8):97-105.
- [10] Rubert A and Schaumann P. Structural steel and plane frame assemblies under fire action. *Fire Safety Journal* 1986;10(3):173-84.
- [11] British Steel. The behaviour of multi-storey steel frame buildings in fire. British Steel, Rotherham; 1999.
- [12] Bailey CG and Lennon T. Full scale fire tests on hollow core slabs. *The Structural Engineer* 2008;86(6):33-9.
- [13] Santiago A, da Silva LS, Vaz G, Vila Real P, Lopez AG. Experimental investigation of the behaviour of a steel sub-frame under a natural fire. *Steel and Composite Structures* 2008;8(3):243-64.
- [14] Bisby L, Gales J, Maluk C. A contemporary review of large-scale non-standard structural fire testing. *Fire Science Reviews* 2013;2:1.
- [15] Bazant Z and Cedolin L. *Stability of structures: elastic, inelastic, fracture and damage theories*. World Scientific; 2010.
- [16] Salençon J. *Yield design. Great Britain and the United States: ISTE Ltd and John Wiley and Sons, Inc; 2013.*
- [17] Pham DT. *Yield design based analysis of high rise reinforced concrete walls in fire*. PhD thesis, Paris-Est University. Paris, France; 2014 [in French].
- [18] Pham DT, de Buhan P, Florence C, Heck JV, Nguyen HH. Interaction diagrams of reinforced concrete in fire: a yield design approach. *Engineering Structures* 2015;90:38-47.

[19] Pham DT, de Buhan P, Florence C, Heck JV, Nguyen HH. Yield-design based of high rise concrete walls subjected to fire loading conditions. *Engineering Structures* 2015;87:153-61.

[20] EN1992-1-2. Eurocode 2: Design of concrete structures-Part 1 2: General rules-structural fire design; 2004.

[21] EN1991-1-2. Eurocode 1: actions on structures-Part 1-2: General actions. Actions on structures exposed to fire; 2002.

[22] CIMbéton. Conception des bâtiments d'activités en béton : Murs séparatifs coupe-feu et façades à fonction d'écran thermique en béton. Paris : Centre d'information sur le ciment et ses applications ; 2007.

[23] MSC. Software Corporation. User documentation of MSC Marc; 2007.